METEOROLOGICAL APPLICATIONS
Meteorol. Appl. **24**: 172–179 (2017)
Published online in Wiley Online Library
(wileyonlinelibrary.com) DOI: 10.1002/met.1614

RMetS
Royal Meteorological Society

An investigation of the influence of the southern annular mode on Indian summer monsoon rainfall

Jayanti Pal, Sutapa Chaudhuri,* Arumita Roychowdhury and Debjani Basu

Department of Atmospheric Sciences, University of Calcutta, Kolkata, India

ABSTRACT: The present research was aimed at identifying the influence of the southern annular mode on the Indian summer monsoon (ISM) by investigating the inter-annual as well as seasonal variation in the southern annular mode index (SAMI) and the ISM rainfall. It is shown that each month of the ISM is influenced by the southern annular mode of different months. The association between the June SAMI and July rainfall was found to be significant as well as important. The investigation was carried out with the NCEP/NCAR reanalysis dataset. The result shows that the monsoon rainfall anomaly is significantly and negatively correlated with the SAMI. The influence of the June SAMI is estimated with sea surface temperature (SST), horizontal wind at 850 hPa pressure level, vertical wind and moisture convergence. The result shows the existence of warm sea surface at 30 ° S during high SAMI years which is surmised to control the cross-equatorial flow during the ISM. It was also observed that the enhanced southerly flow over the south of India is divided into two parts. The major flow is observed towards the western Arabian Sea, subsequently turning clockwise and moving towards the western part of India through the north Arabian Sea. The result further shows that an intense ascending motion from the equator to 30 ° N along the western coast coincides with the low rainfall region. These conditions may lead to an enhanced divergence zone over the western and northeastern region of India which, in turn, may result in less rainfall over India.

KEY WORDS Indian summer monsoon; southern annular mode; rainfall; variability; predictability

Received 27 April 2016; Revised 12 July 2016; Accepted 16 July 2016

1. Introduction

The Indian summer monsoon (ISM) characterizes the largest resource of moisture and precipitation over the tropical region (Webster *et al*., 1998). The Indian economy and agriculture is also greatly influenced by the spatial and temporal variations in the Indian summer monsoon rainfall (ISMR). The variability in the precipitation pattern over the tropical belt is controlled by the circulation pattern, the sea surface temperature (SST) and related anomalies (Shukla, 1975; Rao and Goswami, 1988; Yamazaki, 1988; Clark *et al*., 2000). Scientists have also shown that global phenomena such as the El Niño Southern Oscillation (ENSO), the Quasi Biennial Oscillation (QBO) and the Indian Ocean Dipole (IOD) play a significant role in ISMR variability (Webster *et al*., 1999; Ashok *et al*., 2001; Claud and Terray, 2007; Chaudhuri and Pal, 2014). The ENSO is one of the principal modes that influence the variability in the ISMR (Rasmusson and Carpenter, 1982; Shukla and Paolino, 1983; Webster and Yang, 1992). However, some recent studies pointed out a weak relationship between the ENSO and ISMR (Kumar *et al*., 1999; Sarkar *et al*., 2004). Simmonds and Hope (1997) identified a non-linear relationship between El Niño and the Australian monsoon. Mokhov *et al.* (2012) stated that the finding of Simmonds and Hope (1997) is also applicable for the ISM. Ashok *et al.* (2004) observed that among the IOD, the ENSO and the ISM, the IOD acts as a driving factor to adjust the ENSO and ISM relationship showing a reduced impact of the ENSO–ISM relationship based on the phase of the IOD. Kumar *et al.* (2006) pointed out that the relation between El Niño and the ISM is mostly linked with the variation in the central equatorial Pacific. These changing relationships of the ISM with various atmospheric and oceanic parameters may sometimes stimulate other prevailing modes of variability that can influence the precipitation pattern. Studies with high latitude variability show a probable association of the ISM with the North Atlantic Oscillation (NAO) (Dugam *et al*., 1997). That study shows that the boreal winter and spring-time NAO has a significant influence on the ISM. As with the NAO, a flip-flop mass distribution between middle and high latitude in the Southern Hemisphere, named the southern annular mode (SAM), is observed to influence the moisture transport, SST and regional rainfall (Gong and Wang, 1999; Boer *et al*., 2001; Rao *et al*., 2003; Screen *et al*., 2009). Several studies have reported a trend in SAM toward its positive phase, i.e. when pressure over Antarctica is relatively low compared to the pressure over mid-latitudes, the polar vortex intensifies and the circumpolar westerlies increase (Hurrell and van Loon, 1994; Meehl *et al*., 1998; Gong and Wang, 1999; Mo, 2000; Thompson and Wallace, 2000; Thompson *et al*., 2000; Thompson and Solomon, 2002). Remarkable changes in the SAM have been observed in the present climate with a significant positive trend since the mid-1960s (Thompson and Wallace, 2000; Marshall, 2003). Precipitation anomalies in southern and northern Australia have also been observed to be associated with changes in the phases of the SAM (Meneghini *et al*., 2007). A decrease in subsequent precipitation due to preceding SAM anomalies over the Northern Hemisphere reveals that the leading mode has an influence in a wider sense (Nan and Li, 2003; Wu *et al*., 2009). The June southern annular mode index (SAMI) is found to be strongly correlated with the onset phase as well as the propagation period of the ISM (July–August) (Viswambharan and Mohanakumar,

* Correspondence: S. Chaudhuri, Department of Atmospheric Sciences, University of Calcutta, 51/2 Hazra Road, Kolkata – 700 019, India. E-mail: sutapa.chaudhuri@gmail.com

2013). Since the origin of the Asian summer monsoon circulation is in the oceanic region of the Southern Hemisphere, it is important to explore a possible association between the SAM and the summer monsoon over the Indian subcontinent.

The main objective of this study was to identify a possible relation between the SAMI and ISMR. The variability in precipitation was considered in this study to understand the probable link between the SAMI and ISMR. The relation between the SAM and the ISM is observed for the strongest spell of the ISM. The association between the SAMI and ISMR is observed through the variability in atmospheric circulation, SST anomalies and moisture properties.

2. Data and methodology

As the aim of the present study was to identify the influence of the SAMI on the ISMR it was imperative to understand which SAMI would be better for the purpose, as SAMIs are sensitive to the source data. Ho *et al.* (2012) examined a number of SAMIs acquired from several sources. That study strongly recommended the Marshall or Visbeck station based SAMI for hydro-climate exploration during the pre-satellite era (i.e. pre-1979). The present study was carried out from 1957 to 2013 and thus the Marshall SAMI (Marshall, 2003) was considered. The Marshall SAMI is computed using the Gong and Wang (1999) method which has been used in several studies (Silvestri and Vera, 2009; Feng *et al*., 2010). It is essential to understand which data have been considered for meteorological analysis. Mean sea level pressure (MSLP) data were collected from the ERA-40 reanalysis (Uppala *et al*., 2005), the ERA-Interim reanalysis (Berrisford *et al*., 2009; Dee *et al*., 2011) and the National Centers for Environmental Prediction and the National Center for Atmospheric Research (NCEP/NCAR) reanalysis (Kalnay *et al*., 1996) and compared with Marshall indices. The rest of the required meteorological data were collected from the said sources which have been observed to be compatible with the Marshall indices. The SST data were taken from National Oceanic and Atmospheric Administration (NOAA) Extended Reconstructed Sea Surface Temperature Version 4 (Liu *et al*., 2015), monthly data available on global 2×2 grids that were improved to Version 4 from Version 3b. A non-parametric Spearman's rank correlation and linear correlation have been implemented to identify the association between the SAMI and ISMR. The significance test of the correlations was also carried out using a *t* test. The correlation was confirmed by applying the two-tailed test at the 95% significance level (Wang *et al*., 2005). The 10 year moving average was computed to understand the decadal variability as well as the frequency of epochs in ISMR. The composite difference between a positive SAMI (8 years) and a negative SAMI (8 years) was also used to identify a relation between the SAMI and ISMR. The positive and negative SAMI years are classified on the basis of ± 1 standard deviation from mean June SAMI during the period from 1957 to 2013. Based on the numerical value of the SAMI for a nearly 57 year period, the years 1967, 1979, 1980, 1982, 1989, 2006, 2008 and 2010 were selected as high SAMI years and 1962, 1964, 1977, 1985, 1988, 1992, 1994 and 2003 as low SAMI years (Table 1). The composite and statistical analyses were implemented on the meteorological parameters of wind, moisture and SST to observe the influence of the SAMI on the ISMR.

Table 1. High and low southern annular mode index (SAMI) years based on the Marshall SAMI.

June SAMI			
Positive	Rain anomaly (%)	Negative	Rain anomaly (%)
1967	2.5	1962	−5.1
1979	−16	1964	12.6
1980	1	1977	13.2
1982[a]	**−23.1**	1985	−5.6
1989[b]	**5.1**	**1988**[b]	**26.6**
2006	−2	1992	−19.1
2008	−16.5	1994	20.8
2010	2.8	2003	6.5

[a]Marked year is El Niño year.
[b]Marked years are La Niña years.
The values in El Niño and La Niña years are made bold.

3. Results

Ho *et al.* (2012) used the NOAA index (Thompson and Wallace, 2000) which includes numerical weather prediction model products and satellite observations as reference indices for comparing other SAMIs. The study by Ho *et al.* (2012) suggested that the Marshall and Visbeck data are station based data from the Southern Hemisphere and can be used to estimate the variability in any hydro-climatic condition.

The present study therefore adopts the Marshall SAMI as the reference index and the analyses were carried out initially by comparing the SAMI from the ERA-40, ERA-Interim and NCEP/NCAR with the Marshall index. The SAMIs from the ERA-40, ERA-Interim and NCEP/NCAR were computed following the Gong and Wang method (Gong and Wang, 1999). The SAMI is thus defined in this study as the difference between the normalized zonal MSLP at 40 ° S and 65 ° S. The SAMI is estimated for the total time series available for each dataset and then compared with the Marshall index over the period.

Hydro-climatic studies are nevertheless focused on sub-seasonal timescales, where monthly and weekly information on climatic states are needed for historical review as well as for forecasts. It is therefore imperative to evaluate the monthly SAMI as well. A comparison between the three SAMIs and the Marshall index is carried out with scatter plots of the normalized SAMI values against the normalized Marshall index. The monthly SAMI values were plotted against the corresponding monthly Marshall index value (Figure 1). The SAMI obtained from the ERA-40, ERA-Interim and NCEP/NCAR reanalyses is plotted against the Marshall SAMI during the periods from 1958 to 2002 (Figure 1(a)), 1980 to 2014 (Figure 1(b)) and 1957 to 2014 (Figure 1(c)) respectively. It is apparent from the results that the higher values of the Marshall SAMI are associated with a higher value of the ERA-40 and NCEP/NCAR SAMIs. Hence, a linear association can be established between the Marshall SAMI and the ERA-40 SAMI as well as the NCEP/NCAR SAMI. The SAMI obtained from the ERA-Interim data shows no such linear relationship. The result shows that if the association between the SAMI and hydro-climatic variability at a specified location has to be demonstrated then analogous consequences can be observed with the Marshall, ERA-40 and NCEP/NCAR SAMIs whereas quite different results are observed with the ERA-Interim data. The correlation between the Marshall SAMI and the SAMI obtained from the three sources was estimated during the period from 1980 to 2001 (Table 2). The correlation for the total time series available for the three sources was also computed. The result shows that the correlation is high with ERA-40 and NCEP/NCAR reanalyses during 1980–2001. The correlation is observed to decrease more with ERA-40 than NCEP/NCAR when the total time period is considered. A maximum data length is available for the NCEP/NCAR reanalysis.

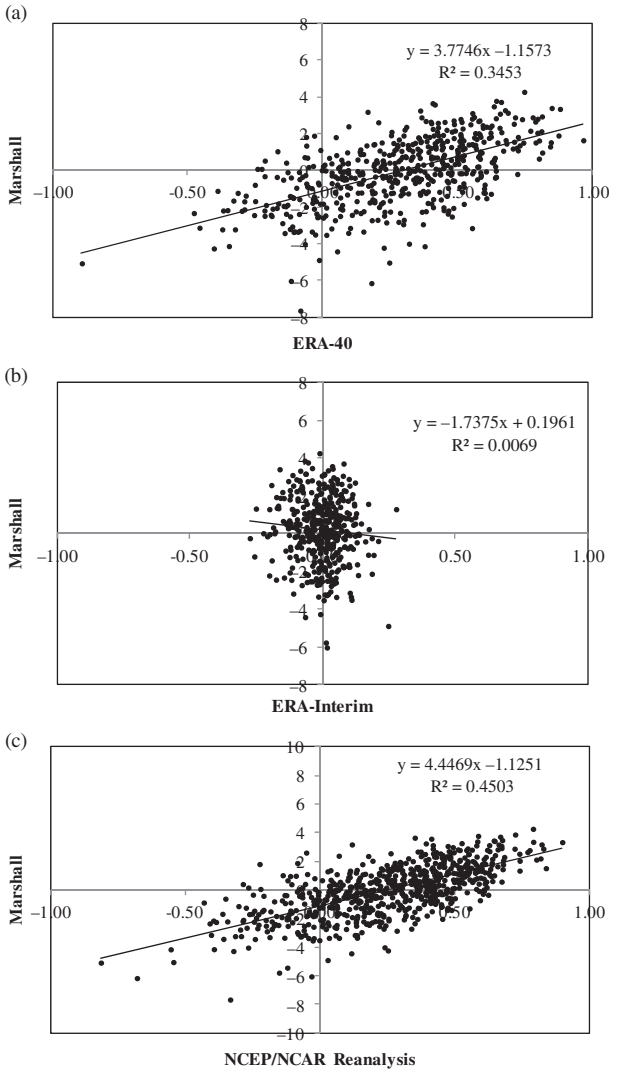

Figure 1. Monthly southern annular mode index (SAMI) values plotted against the monthly Marshall index for (a) ERA-40, (b) ERA-Interim and (c) NCEP/NCAR reanalysis.

Table 2. Correlation between the Marshall southern annular mode index (SAMI) and the SAMI obtained from the other three sources for the time period 1980–2001, full time series.

Temporal span of correlation	ERA-40 (1958–2002)	ERA-Interim (1980–2014)	NCEP/NCAR (1957–2014)
1980–2001	**0.73**	−0.12	**0.72**
Full series	**0.59**	−0.08	**0.67**
Number of years in the full series	44	34	57

The table also includes data length, i.e. the time length of the full time series. Bold values are statistically significant at the 95% level.

Hence, for classification of positive and negative years, the correlation analysis was carried out for the meteorological as well as spatial observations. The NCEP/NCAR reanalysis data are considered in this study. Figure 2 shows the Spearman and linear correlation between the monthly SAMI and the monthly rainfall anomaly (in %) of the ISM. The Spearman rank correlation shows that the rainfall anomaly in June is positively associated with the February SAMI whilst negatively associated with the

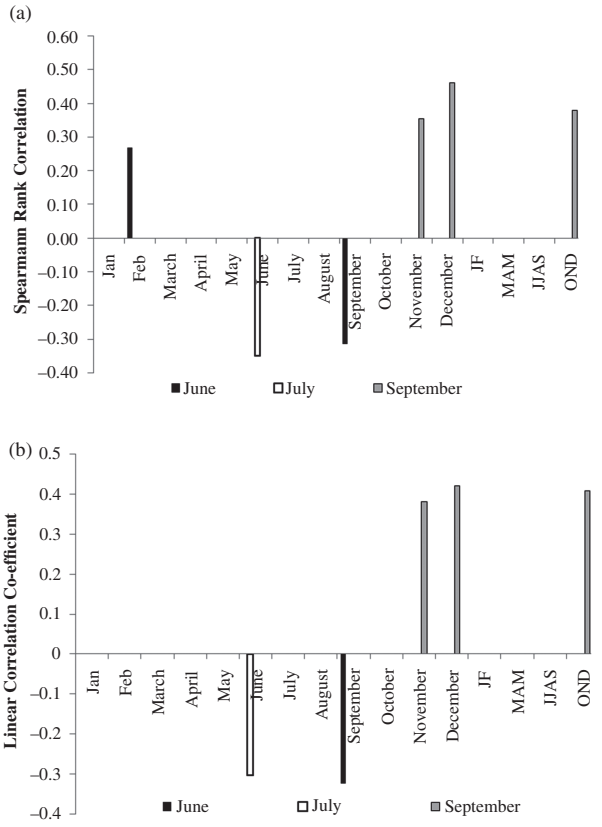

Figure 2. (a) Spearman rank correlation and (b) linear correlation between the Marshall southern annular mode index (SAMI) and the monthly rainfall anomaly of the Indian summer monsoon. Only correlation significant at the 95% level has been plotted here. August month does not possesses any significant correlation.

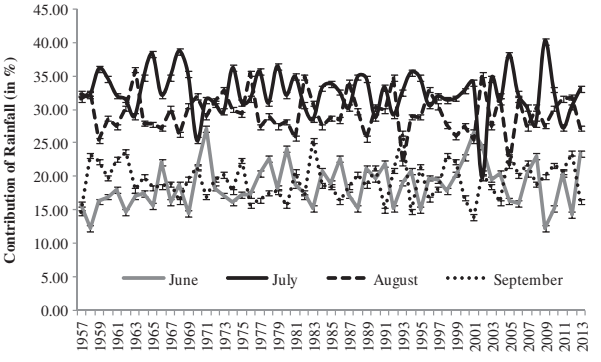

Figure 3. Percentage of the contribution of each month's rainfall to the seasonal rainfall of the Indian summer monsoon.

September SAMI (Figure 2(a)). In July, the rainfall anomaly is observed to be inversely linked to the June SAMI. No association was observed in August. In September, the rainfall anomaly is observed to correlate positively with October, November and the averaged October–November–December SAMI. The correlations obtained are found to be statistically significant at the 95% confidence level. The linear correlation analysis also provides similar results except for the association between the June rainfall anomaly and the February SAMI (Figure 2(b)). It is suggested that June rainfall may have been influenced by the February SAMI through the linear mode whereas other associations are valid in both cases (linear and non-linear mode). The

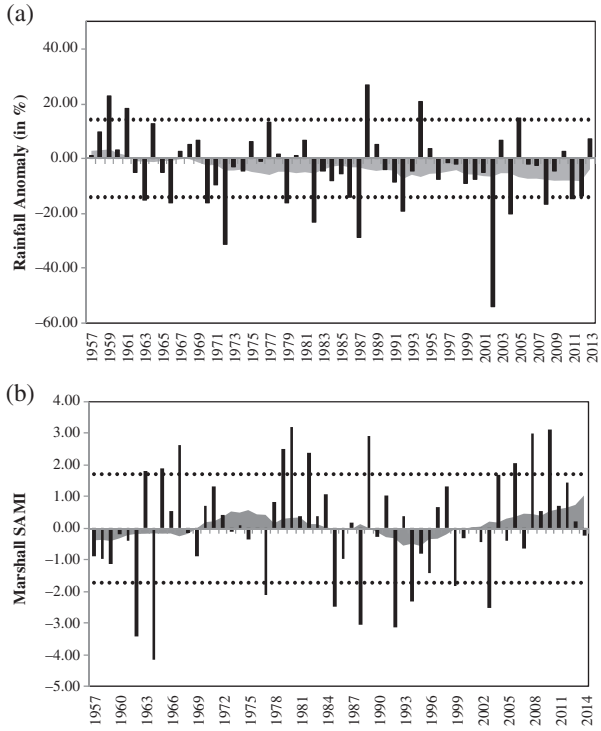

Figure 4. Time series of (a) the July rainfall anomaly (in %) and (b) the Marshall southern annular mode index (SAMI) during June along with 10 year moving averages (filled curve) from 1957 to 2013.

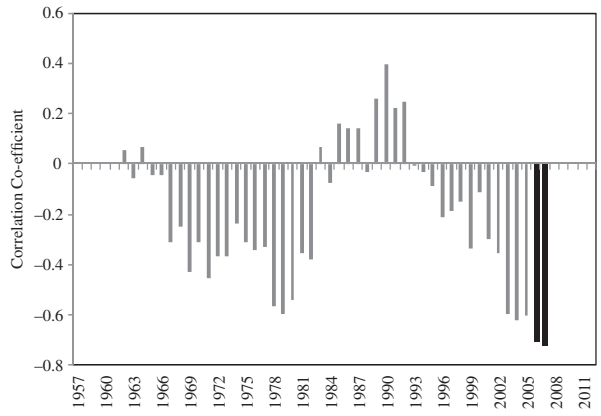

Figure 5. Inter-decadal variability of the 10 year sliding window correlation between the June southern annular mode index (SAMI) and the July rainfall anomaly for 1957–2013.

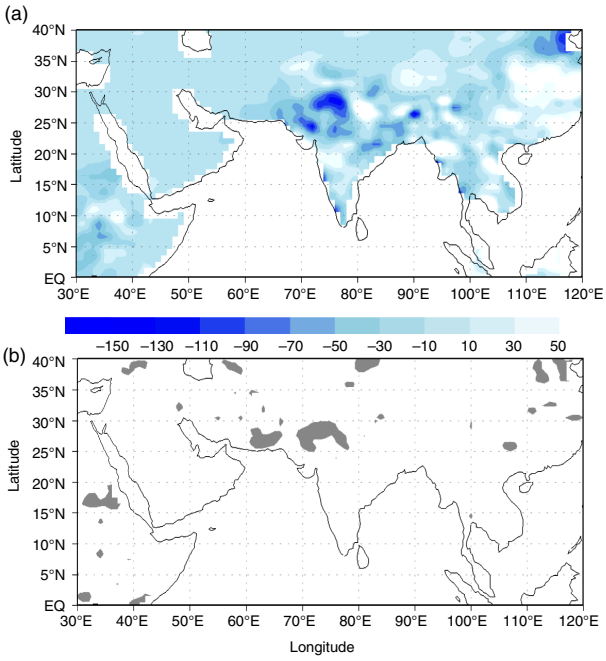

Figure 6. (a) Composite difference of rainfall (in mm) between high and low June southern annular mode index (SAMI) during July. (b) The t value distribution for estimating the difference. Only the statistically significant area has been shaded. [Colour figure can be viewed at wileyonlinelibrary.com].

contribution of each month to seasonal rainfall was estimated as a percentage to identify the important association to be assessed (Figure 3). The monthly analysis shows that July and August contributed more than July and September to seasonal rainfall. As August does not show any association with the SAMI, the present study focuses on the association between the rainfall of July and the June SAMI. Figure 4(a) illustrates the time series of the rainfall anomaly during July, from 1957 to 2013. A large inter-annual variability in rainfall anomaly is observed. The solid filled line indicates the 10 year moving average of the rainfall anomaly. The result shows a steady decrease in the rainfall anomaly and a negative trend in the decadal moving average values after 1960. A similar result with the June SAMI shows a large inter-annual variability (Figure 4(b)). A periodic behaviour in the epoch of the June SAMI is noticed. The result shows a steady increase in the present decade. High and low June SAMI years are classified above and below one standard deviation in order to understand the variability in ISMR during July. A list of high and low SAMI years was prepared (Table 1). The list detects 1982 as a strong El Niño year whereas 1989 and 1988 are strong La Niña years based on the Ocean Niño Index. Only the extreme cases are considered in this study. It is observed from Table 1 that, among 6 years of high June SAMI (excluding El Niño and La Niña years), only 3 years show a negative rainfall anomaly, while in the case of low June SAMI, 4 years manifest a positive rainfall anomaly in 7 years. During a high SAMI period, although positive rainfall anomalies were observed in July, extreme cases associated with a negative rainfall anomaly were observed to exceed them in magnitude. The results show that, in 1982, which is an El Niño year, the rainfall anomaly is highly negative, while in 1989, which is associated with La Niña, it is observed to have a higher rainfall but not exceeding the extreme cases associated with high SAMI years. A maximum positive rainfall anomaly associated with low SAMI years is observed in 1988 which is also associated with La Niña. Thus, in analysing the data, the El Niño and La Niña years have been removed from the composite analysis. This is because the high SAMI associated with El Niño may lead to drought-like conditions over India whereas with La Niña the rainfall may be within the normal range. A reverse situation was observed in the case of a low SAMI. The inter-decadal variability and the association between rainfall and SAMI show alternate phases of negative and positive correlation with a 10 year sliding window analysis (Figure 5) (Foster *et al.*, 2005). The result shows a positive correlation having a magnitude of 0.6 with statistical significance in the first phase whereas the positive correlation is not statistically significant in the second phase. In recent decades the correlation between the SAMI and rainfall is observed to be negative having a magnitude of 0.7 and statistically significant

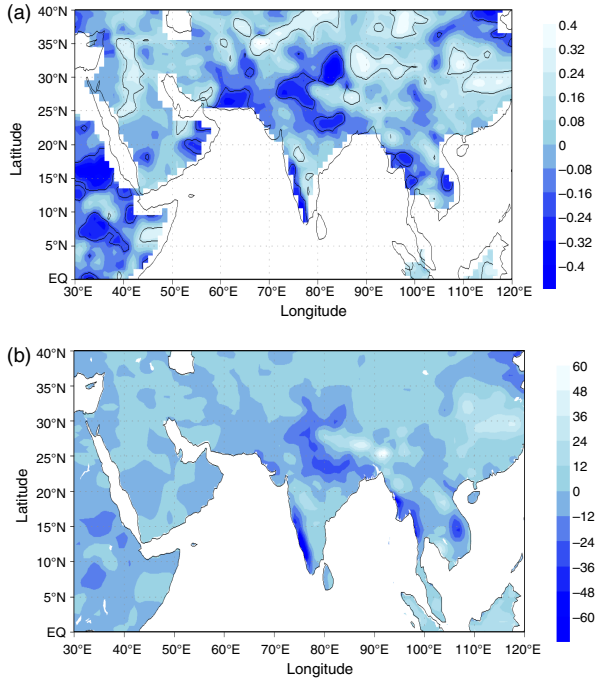

Figure 7. (a) Correlation of the July rainfall anomaly with the June southern annular mode index (SAMI) and (b) the regression of the July rainfall anomaly (in mm) against the June SAMI for 1957–2013. The contoured correlation depicts statistical significance at the 95% level. [Colour figure can be viewed at wileyonlinelibrary.com].

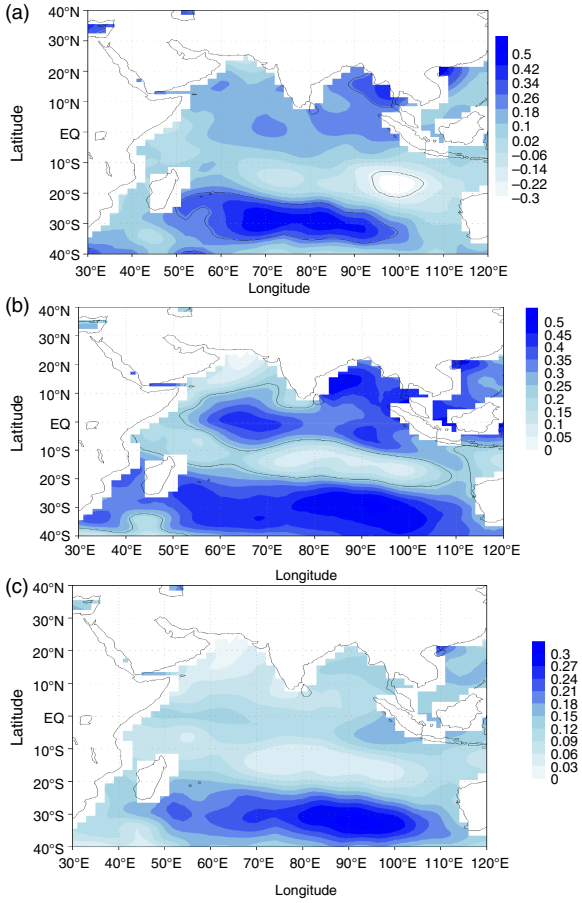

Figure 8. (a) Composite difference of sea surface temperature (SST) (in °C) between high and low June southern annular mode index (SAMI) during July and (b) correlation between July SST anomaly and June SAMI; (c) regression of July SST (in °C) against June SAMI. The contoured area in the difference and correlation plots depicts statistical significance at the 95% level. [Colour figure can be viewed at wileyonlinelibrary.com].

at the 95% confidence level. The composite difference between high and low June SAMI years during July (Figure 6(a)) shows a negative rainfall anomaly over the region of the monsoon trough during high June SAMI years. The negative anomalies are stronger between 25 ° N and 30 ° N latitudes along the northwestern region and also the southwest coast. It is further observed that some parts of the northeast coastal region that fall under the southern part of the monsoon trough also encounter a lower rainfall anomaly during high June SAMI years. This result shows that strong positive anomalies occur over some part of northeast India and a strong positive signal appears near 27 ° N; 81 ° E. The difference is statistically significant at the 95% confidence level over the region of strong negative anomaly (Figure 6(b)). The correlation between the June SAMI and July ISMR anomaly was estimated for the period from 1957 to 2013 (Figure 7(a)). The figure depicts that the June SAMI is negatively correlated with the July ISMR over most of India. Areas of significant negative correlations were observed between the latitude belts of 21 ° N and 30 ° N along the monsoon trough region and also over the southwest sector of India whilst significant positive correlations were noticed over northeast India and near the region around 18 ° N, 75 ° E. The regression of the rainfall anomaly during 1957–2013 onto the SAMI was estimated (Figure 7(b)). The result shows a quite similar spatial distribution to that obtained from composite difference and correlation analyses. An intense positive anomaly zone is observed over the northeastern region and around 18 ° N, 75 ° E while a negative anomaly is observed along the monsoon trough and southwestern coast of India. The SST variability over the Indian Ocean has been linked with the SAM (Yeo and Kim, 2015). Therefore, assessment of the composite difference of the SST between high and low June SAMI years is important to identify the internal linkage between monsoon circulation and the SAMI. The result shows an intense warming of 0.4 °C around 30 ° S and cooling of 0.3 °C at 15 ° S (Figure 8(a)). The eastern Bay of Bengal (BOB) is also observed to show warming of above 0.2 °C. However, the northern part of the Arabian Sea and the Somali coast was observed to have a cooling of 0.1 °C. A significant positive correlation between the SST anomaly and the SAMI was observed over the southern and equatorial Indian Ocean and the BOB (Figure 8(b)). The regression of SST onto the SAMI implies a positive anomaly all over the region; however, the magnitude varies from place to place (Figure 8(c)). The result shows a higher magnitude of change in SST at around 30 ° S. The circulation pattern at the 850 hPa level in July is an important feature. It is observed that during high SAMI years the cross-equatorial flow was disrupted in July (Figure 9(a)). The result shows an enhancement of the southerly flow at the equator which strikes the southern peninsula. Instead of penetrating to India it divides into two branches. It has also been observed that the enhanced southerly flow over the south of India is separated into two parts. The chief flow is observed towards the western Arabian Sea which subsequently turns clockwise and moves towards the western part of India through the north Arabian Sea, and the other part of the wind approaches the BOB as a weak flow. One anomalous flow towards the eastern BOB and thus the Somali coast may affect the actual monsoon circulation. An inflow was observed over the north Arabian Sea which travels towards western India. The results further show that during high SAMI years a

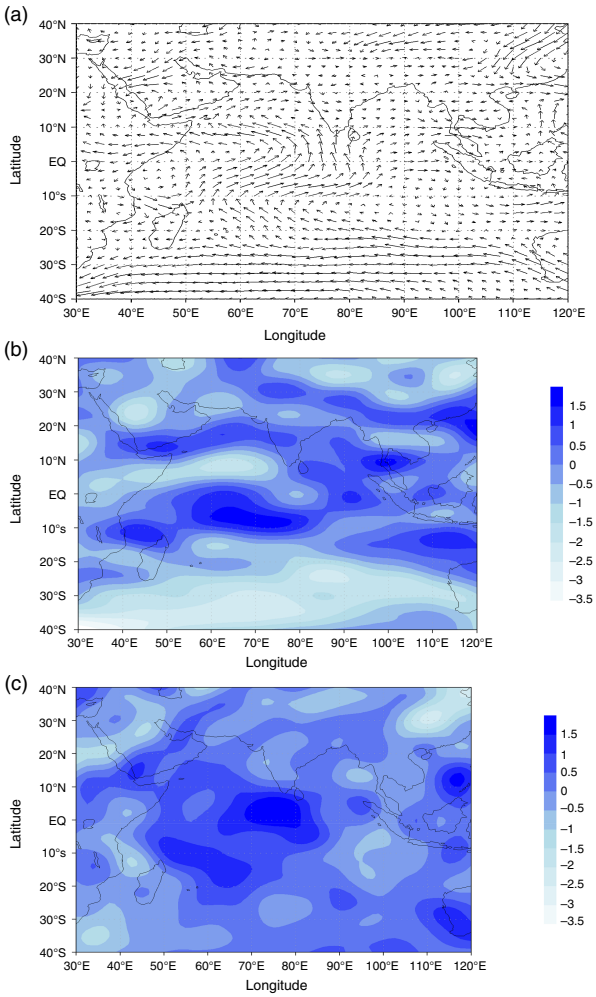

Figure 9. Composite difference of (a) vector wind, (b) zonal wind and (c) meridional wind at 850 hPa between high and low June southern annular mode index (SAMI) during July. The wind is in m s^{-1}. [Colour figure can be viewed at wileyonlinelibrary.com].

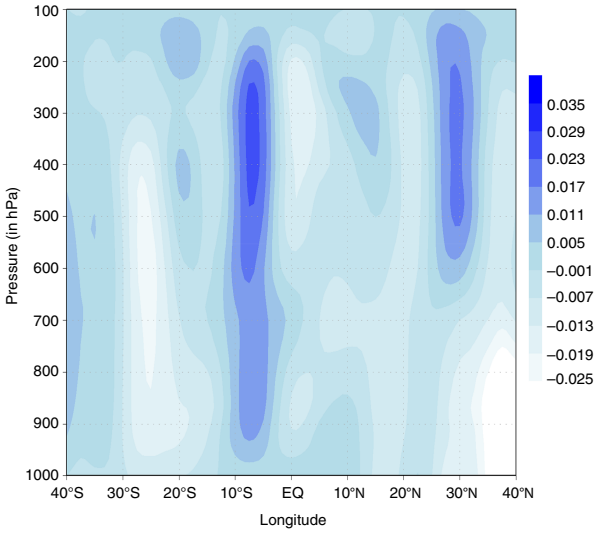

Figure 10. Vertical profile of the composite difference of the vertical velocity (Pa s^{-1}) between high and low June southern annular mode index (SAMI) years during July. [Colour figure can be viewed at wileyonlinelibrary.com].

strong zonal flow was observed over the equatorial region mainly around 10 ° S, the BOB and the central Arabian Sea, while the meridional structure was found to be strong at the Equator, near the southern tip of India (Figure 9(b)). The strong meridional structure can be attributed to enhancement of the southerly flow (Figure 9(c)). The vertical profile of the vertical velocity was computed for the longitude belt 70–80 ° E. The vertical velocity difference shows an enhanced ascending motion between 40 ° S and 12 ° S, in which the increase in magnitude is high at 900 hPa and between 600 and 500 hPa (Figure 10). The results further show an enhanced ascending motion from the Equator to 30 ° N in which the increase in magnitude is high in the upper troposphere. The abnormal downward wind flow is observed to be increased between the Equator and 10 ° S in the Southern Hemisphere whereas in the Northern Hemisphere the latitude belt between 30 ° and 40 ° N manifests intense descending motion with higher magnitude between the 500 and 400 hPa pressure levels. It is noted that the latitudinal belt under a warm SST encounters an intense ascending motion and the region of lower rainfall manifests an intense descending motion. The warm SST and anomalous horizontal flow may disturb moisture transport over India. The moisture convergence at this level was therefore analysed to understand the moisture transport at the 850 hPa level (Figure 11). The results show that during high SAMI years a strong divergence zone was identified over western and north-eastern regions over India and near the Somali coast of Africa (Figure 11(a)) whereas a convergence zone was observed over the eastern coast along the latitude at 10 ° N. However, during low SAMI years the convergence over India becomes very strong and the divergence zone weakens (Figure 11(b)). The result thus reveals an inverse relation between the June Marshall SAMI and July ISMR. The epochal variation also shows a negative association except for the decade 1990–2000. The high SAMI years do not occur within this decade but two low SAMI years are included. The composite and statistical analyses show that the June SAMI may have a reverse relation with rainfall over the monsoon trough. A warm sea surface, disrupted cross-equatorial flow and increased divergence were observed to be significant features of high June SAMI years.

4. Summary and discussion

The present study investigated the impact of the southern annular mode (SAM) on the Indian summer monsoon (ISM) by analysing the inter-annual variation of the southern annular mode index (SAMI) and the ISM rainfall (ISMR) anomaly in percentage. The study compared ERA-40, ERA-Interim and NCEP/NCAR reanalysis data against the Marshall SAMI. It shows that the NCEP/NCAR reanalysis gives relatively better data for evaluating the influence of the SAM on the Indian hydro-climate along with the Marshall SAMI. The results of the study demonstrate that monsoon months are influenced by the SAM of dissimilar months. Coalition between June SAMI and July rainfall has been found to be noteworthy as well as imperative among all of the alliances. The study shows that July is a significant month to be influenced by SAM due to its higher contribution in ISM season. The classification of high and low SAMI was made based on the Marshall SAMI. It is vital to identify whether the disparity is a consequence of El Niño, which is a dominant mode of variability and believed to be one of the inversely correlated parameters of the ISM in the context of the observed association between the SAMI and the ISMR (Rasmusson and Carpenter, 1982; Shukla and Paolino, 1983; Webster and Yang, 1992; Kumar *et al.*,

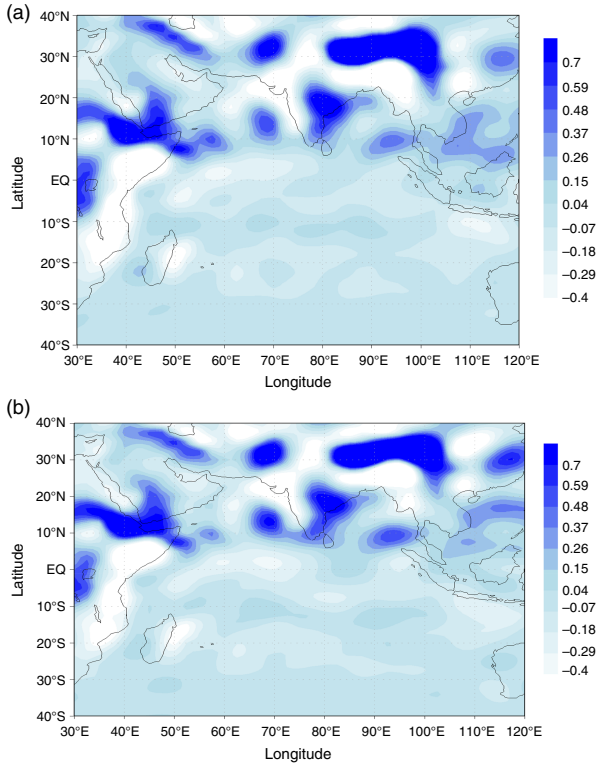

Figure 11. Composite moisture convergence (g kg^{-1} s^{-1}) during (a) high June southern annular mode index (SAMI) years and (b) low June SAMI years. [Colour figure can be viewed at wileyonlinelibrary.com].

2006). In the study an amplification of the effect of the SAMI is observed associated with El Niño and La Niña. To reduce the effect of El Niño and La Niña, strong or extreme event years were removed in the present study. Surveillance illustrates a reverse relation between July rainfall and the June SAMI. The decadal variability demonstrates a sinusoidal pattern in the June SAMI. In the recent decade a steady increase was observed. A trend toward its positive phase over recent decades has been reported in several studies (Thompson *et al*., 2000; Marshall *et al*., 2004; Marshall, 2007). It has been suggested that the present trend is due to human activity, stratospheric ozone depletion and amplified greenhouse gas concentrations (Cai and Watterson, 2002; Gillett and Thompson, 2003; Marshall *et al*., 2004; Shindell and Schmidt, 2004; Arblaster and Meehl, 2006; Cai and Cowan, 2006; Miller *et al*., 2006). The present study attempted to examine whether this trend has influenced the ISM. The correlation analyses show that both linear and non-linear associations are present between the SAMI and ISMR. It is observed that western India, mainly Rajasthan and the southwest coast of India, encounter lower rainfall whereas the northeast and east coast of India manifest higher rainfall. The effect of the SAM is thus not uniform over India. A attempt was therefore made to evaluate a link with sea surface temperature (SST), horizontal wind at 850 hPa pressure level, vertical wind and moisture convergence. The result shows that the SST is an important parameter for the present study (Hall and Visbeck, 2002; Sen Gupta and England, 2006; Verdy *et al*., 2006; Ciasto and Thompson, 2008; Screen *et al*., 2009). It has been observed that the SAM can be modified by induced SST anomalies through positive feedback (Sen Gupta and England, 2007). An increase in SST at 30 ° S and cooling at 10 ° S over the southwest Indian Ocean was observed during high SAMI years. Yeo and Kim (2015) observed SST variability in the Southern Hemisphere due to a change in spatial structure of the SAM. Although the magnitude of the correlation between the SAMI and the SST was observed to be low, a correlation above 0.25 shows significant association that suggests warming over the southern Indian Ocean, equatorial Indian Ocean and Bay of Bengal. The enhanced southerly flow over the equatorial Indian Ocean may disrupt low level summer monsoon flow. The flow at 850 hPa is observed to split at the south of India and the main flow travels towards the western Arabian Sea and subsequently spins clockwise and starts travelling towards western India through the north Arabian Sea. Viswambharan and Mohanakumar (2013) suggested that the wind at 850 hPa over south India has weakened during the difference in the high and low SAMIs in June. An intense ascending motion from the equator to 30 ° N along the western coast coincides with the low rainfall region. These conditions may lead to an enhanced divergence zone over the western and northeastern region that may in turn result in less rainfall over India. The study thus shows a significant relationship between the SAMI and the ISMR. Viswambharan and Mohanakumar (2013) have also analysed the association between the SAMI and the ISMR and found that a high SAMI during June is not conducive for precipitation over most parts of India during July–August. That study also removed the effect of El Niño by performing a partial correlation; however, while the composite analysis was considered all El Niño and La Niña years were included. Thus, the features associated with high and June SAMI may have an El Niño and La Niña effect. The present study could not find any correlation between the SAMI and the rainfall anomaly for August. The consideration of August is not required. The study depicts a reduced convergence along with intense ascending motion between longitude belts 70–80 ° E. The reduction in rainfall during high SAMI has been explained while increased precipitation over the northeast region was not understood. External or internal sources of forcing may act as a catalyst for the increase which is not considered in this study.

Acknowledgement

The corresponding author Sutapa Chaudhuri acknowledges the Ministry of Earth Science, Government of India and the Monsoon Mission Directorate, Indian Institute of Tropical Meteorology, Pune, India, for providing the opportunity to join the National Monsoon Mission. The authors thank the anonymous reviewers and the Editor of the journal for constructive comments and suggestions.

References

Arblaster MJ, Meehl GA. 2006. Contributions of external forcings to southern annular mode trends. *J. Clim.* **19**: 2896–2905.

Ashok K, Guan Z, Saji NH, Yamagata T. 2004. On the individual and combined influences of the ENSO and the Indian Ocean dipole on the Indian summer monsoon. *J. Clim.* **17**: 3141–3155.

Ashok K, Guan Z, Yamagata T. 2001. Impact of the Indian Ocean dipole on the relationship between the Indian monsoon rainfall and ENSO. *Geophys. Res. Lett.* **28**: 4499–4502.

Berrisford P, Dee DP, Fielding K, Fuentes M, Kallberg P, Kobayashi S, Uppala SM. 2009. The ERA-Interim archive. ERA Report Series No. 1, ECMWF: Reading. http://www.ecmwf.int/publications (accessed 1 October 2011).

Boer GJ, Fourest S, Yu B. 2001. The signature of the annular modes in the moisture budget. *J. Clim.* **14**: 3655–3665.

Cai W, Cowan T. 2006. SAM and regional rainfall in IPCC AR4 models: Can anthropogenic forcing account for southwest Western

Australian winter rainfall reduction? *Geophys. Res. Lett.* **33**: L24708, DOI: 10.1029/2006GL028037.
Cai W, Watterson I. 2002. Modes of interannual variability of the Southern Hemisphere circulation simulated by the CSIRO climate model. *J. Clim.* **15**: 1159–1174.
Chaudhuri S, Pal J. 2014. The influence of El Niño on the ISM rainfall anomaly: a diagnostic study of the '82/83 and '97/98 events. *Meteorol. Atmos. Phys.* **124**: 183–194.
Ciasto LM, Thompson DW. 2008. Observations of large-scale ocean–atmosphere interaction in the southern hemisphere. *J. Clim.* **21**: 1244–1259.
Clark CO, Cole JE, Webster PJ. 2000. Indian Ocean SST and Indian summer rainfall: predictive relationship and their decadal variability. *J. Clim.* **13**: 2503–2519.
Claud C, Terray P. 2007. Revisiting the possible links between the quasi-biennial oscillation and the ISM using NCEP R-2 and CMAP fields. *J. Clim.* **20**: 773–787.
Dee DP, Uppala SM, Simmons AJ, Berrisford P, Poli P, Kobayashi S, *et al.* 2011. The ERA-Interim reanalysis: configuration and performance of the data assimilation system. *Q. J. R. Meteorol. Soc.* **137**: 553–597.
Dugam SS, Kakade SB, Verma RK. 1997. Inter-annual and long-term variability in the North Atlantic Oscillation and ISM rainfall. *Theor. Appl. Climatol.* **58**: 21–29.
Feng J, Li J, Li Y. 2010. Is there a relationship between the SAM and southwest Western Australian winter rainfall? *J. Clim.* **23**: 6082–6089.
Foster J, Bevis M, Businger S. 2005. GPS Meteorology: sliding-window analysis. *J. Atmos. Oceanic Technol.* **22**: 687–695.
Gillett N, Thompson D. 2003. Simulation of recent southern hemisphere climate change. *Science* **302**: 273–275.
Gong D, Wang S. 1999. Definition of Antarctic oscillation index. *Geophys. Res. Lett.* **26**: 459–462.
Hall A, Visbeck M. 2002. Synchronous variability in the southern hemisphere atmosphere, sea ice, and ocean resulting from the annular mode. *J. Clim.* **15**: 3043–3057.
Ho M, Kiem AS, Verdon-Kidd DC. 2012. The southern annular mode: a comparison of indices. *Hydrol. Earth Syst. Sci.* **16**: 967–982.
Hurrell JW, van Loon H. 1994. A modulation of the atmospheric annual cycle in the Southern Hemisphere. *Tellus* **46A**: 325–338.
Kalnay E, Kanamitsu M, Kistler R, Collins W, Deaven D, Gandin L, *et al.* 1996. The NCEP/NCAR 40-year reanalysis project. *Bull. Am. Meteorol. Soc.* **77**: 437–470.
Kumar KK, Rajagopalan B, Cane MA. 1999. On the weakening relationship between the Indian Monsoon and ENSO. *Science* **284**: 2156–2159.
Kumar KK, Rajagopalan B, Hoerling M, Bates G, Cane M. 2006. Unraveling the mystery of Indian monsoon failure during El Niño. *Science* **113**: 1152.
Liu W, Huang B, Thorne PW, Banzon VF, Zhang HM, Freeman E, *et al.* 2015. Extended reconstructed sea surface temperature version 4 (ERSST.v4): Part II. Parametric and structural uncertainty estimations. *J. Clim.* **28**: 931–951, DOI: 10.1175/JCLI-D-14-00007.1.
Marshall GJ. 2003. Trends in the southern annular mode from observations and reanalyses. *J. Clim.* **16**: 4134–4143.
Marshall GJ. 2007. Half-century seasonal relationships between the southern annular mode and Antarctic temperatures. *Int. J. Climatol.* **27**: 373–383.
Marshall GJ, Stott PA, Turner J, Connolley WM, King JC, Lachlan- Cope TA. 2004. Causes of exceptional atmospheric circulation changes in the southern hemisphere. *Geophys. Res. Lett.* **31**: L14205.
Meehl GA, Hurrell JW, Loon HV. 1998. A modulation of the mechanism of the semiannual oscillation in the southern hemisphere. *Tellus.* **50A**: 442–450.
Meneghini B, Simmonds I, Smith IN. 2007. Association between Australian rainfall and southern annular mode. *Int. J. Climatol.* **27**: 109–121.
Miller RL, Schmidt GA, Shindell DT. 2006. Forced annular variations in the 20th century intergovernmental panel on climate change fourth assessment report models. *J. Geophys. Res.* **111**: D18101.
Mo KC. 2000. Relationships between low-frequency variability in the southern hemisphere and sea surface temperature anomalies. *J. Clim.* **13**: 3599–3610.
Mokhov II, Smirnov DA, Nakonechnv PI, Kozlenko SS, Kurths J. 2012. Relationship between El Niño/southern oscillation and the Indian monsoon. *Izv. Atmos. Oceanic. Phys.* **48**: 47–56.
Nan S, Li J. 2003. The relationship between summer precipitation in the Yangtze River valley and the previous southern hemisphere annular mode. *Geophys. Res. Lett.* **30**(24): 2266.
Rao KG, Goswami BN. 1988. Inter-annual variations of sea surface temperature over the Arabian Sea and the Indian monsoon: a new perspective. *Mon. Weather Rev.* **116**(3): 558–568.
Rao VB, Do Carmo AMC, Franchito SH. 2003. Inter-annual variations of storm tracks in the southern hemisphere and their connections with the Antarctic oscillation. *Int. J. Climatol.* **23**: 1537–1545.
Rasmusson EM, Carpenter TH. 1982. Variations in tropical sea surface temperature and surface wind fields associated with the southern oscillation/El Niño. *Mon. Weather Rev.* **110**: 354–384.
Sarkar S, Singh RP, Kafatos M. 2004. Further evidences for the weakening relationship of Indian rainfall and ENSO over India. *Geophys. Res. Lett.* **31**: L13209, DOI: 10.1029/2004GL020259.
Screen JA, Gillet NP, Stevens DP, Marshall GJ, Roscoe HK. 2009. The role of eddies in the southern ocean temperature response to the southern annular mode. *J. Clim.* **22**: 805–818.
Sen Gupta A, England MH. 2006. Coupled ocean–atmosphere–ice response to variations in the southern annular mode. *J. Clim.* **19**: 4457–4486.
Sen Gupta A, England MH. 2007. Coupled ocean–atmosphere feedback in the southern annular mode. *J. Clim.* **20**(14): 3677–3692.
Shindell DT, Schmidt GA. 2004. Southern hemisphere climate response to ozone changes and greenhouse gas increases. *Geophys. Res. Lett.* **31**: L18209.
Shukla J. 1975. Effect of Arabian sea-surface temperature anomaly on Indian summer monsoon: a numerical experiment with the GFDL model. *J. Atmos. Sci.* **32**: 503–511.
Shukla J, Paolino DA. 1983. The southern oscillation and the long-range forecasting of summer monsoon rainfall over India. *Mon. Weather Rev.* **111**: 1830–1837.
Silvestri G, Vera C. 2009. Nonstationary impacts of the southern annular mode on Southern Hemisphere climate. *J. Clim.* **22**: 6142–6148.
Simmonds I, Hope P. 1997. Persistence characteristics of Australian rainfall anomalies. *Int. J. Climatol.* **17**: 597–613.
Thompson DWJ, Solomon S. 2002. Interpretation of recent Southern Hemisphere climate change. *Science* **296**: 895–899.
Thompson DWJ, Wallace JM. 2000. Annular modes in the extratropical circulation. Part I: month-to-month variability. *J. Clim.* **13**: 1000–1016.
Thompson DWJ, Wallace JM, Hegerl GC. 2000. Annular modes in the extratropical circulation. Part II. *Trends. J. Clim.* **13**: 1018–1036.
Uppala SM, Kallberg PW, Simmons AJ, Andrae U, Da Costa BV, Fiorino M, *et al.* 2005. The ERA-40 re-analysis. *Q. J. R. Meteorol. Soc.* **131**: 2961–3012.
Verdy A, Marshall J, Czaja A. 2006. Sea surface temperature variability along the path of the Antarctic Circumpolar Current. *J. Phys. Oceanogr.* **36**(7): 1317–1331.
Viswambharan N, Mohanakumar K. 2013. Signature of a southern hemisphere extratropical influence on the summer monsoon over India. *Clim. Dyn.* **41**: 367–379.
Wang D, Wang C, Yang X, Lu J. 2005. Winter northern hemisphere surface air temperature variability associated with the Arctic Oscillation and North Atlantic Oscillation. *Geophys. Res. Lett.* **32**: L16706.
Webster PJ, Magana VO, Palmer TN, Shukla J, Tomas RA, Yanai M, *et al.* 1998. Monsoons: processes, predictability, and the prospects for prediction. *J. Geophys. Res.* **103**: 14451–14510.
Webster PJ, Moore A, Loschnigg J, Leban M. 1999. Coupled ocean dynamics in the Indian Ocean during 1997–1998. *Nature* **401**: 356–360.
Webster PJ, Yang S. 1992. Monsoon and ENSO: selectively interactive systems. *Q. J. R. Meteorol. Soc.* **118**: 877–926.
Wu Z, Li J, Wang B, Liu X. 2009. Can the southern hemisphere annular mode affect China winter monsoon? *J. Geophys. Res.* **114**: D11107.
Yamazaki K. 1988. Influence of sea surface temperature anomalies over the Indian Ocean and Pacific Ocean on the tropical atmospheric circulation – a numerical experiment. *J. Meteorl. Soc. Jpn.* **66**: 797–806.
Yeo SR, Kim KY. 2015. Decadal changes in the Southern Hemisphere sea surface temperature in association with El Niño–Southern Oscillation and Southern Annular Mode. *Clim. Dyn.* **45**:(11): 3227–3242, DOI: 10.1007/s00382-015-2535-z.

